Modeling the Nucleation and Crystallization Kinetics of a Palm Stearin/Canola Oil Blend and Lard in Bulk and Emulsified Form

Shawn D. Campbell[a], H. Douglas Goff[a], and Dérick Rousseau[b,*]

[a]Department of Food Science, University of Guelph, Guelph, Ontario, Canada N1G 2W1, and [b]School of Nutrition, Ryerson University, Toronto, Ontario, Canada, M5B 2K3

ABSTRACT: Using high-pressure homogenization to generate different droplet size distributions, the nucleation and crystallization of two fat systems [lard or a palm stearin/canola oil blend (PSCO)] were compared in bulk and emulsified form. Droplet size reduction decreased the final volume fraction of solid fat primarily in the lard system vs. the PSCO system, with a greater reduction in volume fraction using the homogenization regime that led to smaller droplets. Homogeneous and heterogeneous models showed that the nucleation rate generally decreased with a reduction in droplet size. However, the Gibbs surface energy (γ) was significantly underestimated using the homogeneous model, whereas the heterogeneous model fit the data adequately ($P < 0.05$). The temperature sensitivity of the calculated impurity concentration in all emulsified systems was droplet size dependent. The Avrami model showed the emulsified fats to have lower Avrami indices relative to the bulk fat as well as lower crystallization rate constants. Differences in the Avrami indices and the rate constants were more pronounced in the bulk and emulsified PSCO compared with lard.

Paper no. J10474 in *JAOCS 81*, 213–219 (March 2004).

KEY WORDS: Crystallization, heterogeneous, homogeneous, modeling, nucleation, triacylglycerols.

The triacylglycerols (TAG) contained in commercial foods are highly variable in composition, and hence in crystallization behavior. Control of the liquid–solid transition in such TAG is crucial for the proper development of microstructure in many foods, namely, those undergoing phase inversion, such as butter, ice cream, and spreads. The thermodynamic equilibrium of solid and liquid fat in a system does not necessarily reflect the pathway taken to achieve its degree of solidification. The crystallization kinetics of fats can be described by their nucleation rates, and these can be described by classical methods incorporating the thermodynamic driving force of the reaction with the frequency term of the reaction (1,2).

However, classical crystallization theories that describe the behavior of bulk fats adequately are not necessarily applicable to dispersed systems, as the mechanism of nucleation can be either homogeneous or heterogeneous. Homogeneous nucleation occurs directly from the melt, in the absence of impurities. Conversely, heterogeneous nucleation occurs in the presence of impurities, *viz.,* high-melting TAG, emulsifiers, dust, and so on (3,4). The prevailing mechanism depends on the degree of undercooling and/or the number of catalytic impurities present at the droplet surface or within its volume (5,6). Surface nucleation can be influenced by impurities, as investigated by Awad *et al*. (7), Kaneko *et al*. (8), and Hodate *et al*. (9), who found that nucleation rates were increased at the interface as a result of added hydrophobic impurities, yet crystal growth was retarded within droplets.

Contrary to bulk systems, dispersed fats are far more likely to undergo homogeneous nucleation as potential impurities are compartmentalized, leading to independent nucleation and crystallization events. Thus, the impact of emulsification on the nucleation kinetics (homogeneous vs. heterogeneous) and crystallization behavior is highly dependent on the composition and purity of the dispersed phase, the degree of dispersion (droplet size distribution), and undercooling. The goal of this research was to determine the applicability of three crystallization models to the solidification behavior of two commercial fat systems in bulk and emulsified form.

MATERIALS AND METHODS

Refined, bleached, and deodorized palm stearin was obtained from CanAmera Foods (Toronto, ON, Canada); lard and canola oil were purchased from a local supermarket. A 60:40 (%, w/w) palm stearin/canola oil (PSCO) blend was prepared by blending the respective fats at 90°C.

The FA compositions of the lard, palm stearin, and canola oil were determined by GLC (10). Analysis by direct-injection GLC revealed that 95% of the TAG were between C_{48} and C_{56}. The compositions were primarily palmitic, stearic, and oleic acids, with some linoleic and linolenic acids in the PSCO blend. The MAG contents of lard and the PSCO blend were 1.0 and 0.2%, respectively, and the DAG contents were 4.1 and 4.4%, respectively. FFA contents of the lard, palm stearin, and canola oil were 0.03, 0.1, and 0.02%, respectively, as determined by AOCS method Ca 5a-40 and expressed as the percentage of oleic acid (w/w) (11).

The emulsions formed in this study were 40% (w/w) oil-in-water emulsions with a consistent surfactant concentration of 1% (w/w) Tween 80 (Quest International, Lachine, PQ,

*To whom correspondence should be addressed.
E-mail: rousseau@ryerson.ca

Canada) dispersed in the continuous phase prior to emulsification. The surfactant polyoxyethylene (20) sorbitan monooleate (Tween 80) (HLB = 15.4) is a water-soluble emulsifier with the oleic acid residue as the predominant R-group (70%). Ingredients were heated to 90°C and emulsified with a Gaulin V15-8T (APV Gaulin, Everett, MA) two-stage valve homogenizer. Two homogenization treatments were used (800/600 and 2500/600 psi), with the second-stage valve set to 600 psi first and the remainder of the pressure applied using the first-stage valve. Lard and PSCO treatments were designated according to homogenization treatment. For example, "lard 800" was a 40% lard emulsion with the 800/600-psi homogenization conditions and "lard 2500" was a 40% lard emulsion with the 2500/600-psi homogenization conditions. The hot samples were stored in glass-vacuum bottles at 70–80°C and tempered to 60°C in a water bath prior to analysis. The droplet size distributions were measured by light scattering, using a Mastersizer X particle size analyzer (Malvern, Worcestershire, United Kingdom). The emulsified samples were dispersed in a small-sample presentation unit using Milli-Q water (R = 18.2 MΩ). In both fat systems, the droplet size distributions generated by the two homogenization treatments were characterized by the most probable droplet radius (r_m) and full width at the half maximum (fwhm) peak value. The 800-psi treatment generated emulsions with fwhm values of 1.264 ± 0.001 μm and r_m of 0.437 ± 0.012 μm for both fat systems, whereas the 2500-psi treatment generated a distribution with an fwhm value of 1.106 ± 0.012 μm and r_m of 0.343 ± 0.003 μm for lard and with an fwhm value of 1.120 ± 0.002 μm and r_m of 0.375 ± 0.002 μm for PSCO. The distributions of fats homogenized at higher pressures were more monodispersed and were shifted to lower droplet sizes (Fig. 1).

Solid fat content was measured with a Bruker Mq pulsed NMR spectrometer (Bruker Canada, Milton, Ontario, Canada) fitted with a temperature-controlled sample chamber. The cell temperature of the water bath-cooled sampling chamber was calibrated over the range of 10 to 30°C by measuring the equilibrium temperature of samples with a thermocouple probe. A sample size of 800 μL, in a capped NMR tube, was used for analyses to accommodate heat transfer and sample equilibration. Bulk samples were preheated to 80°C for 20 min to erase crystal history and then tempered at 60°C prior to analysis. NMR tubes were quenched in a water bath and measured during the cooling period prior to being placed in the temperature-controlled cell for the remainder of the experiment. Equilibration time for samples ranged from 2 to 3 min, depending on the isothermal temperature desired. Data were acquired and analyzed using software provided by the instrument manufacturer.

ANOVA ($\alpha = 0.05$) and linear regression ($\alpha = 0.05$) were performed on the data in SAS v. 6.12 (SAS Institute Inc., Cary, NC), using Proc GLM and Proc Reg, respectively. Particle size distributions and the Avrami model were fitted with SigmaPlot 2000 v. 6.10 (SPSS Inc., Chicago, IL) using a least squares analysis ($\alpha = 0.05$). The homogeneous and the heterogeneous nucleation models were fitted with Mathcad Professional 7 (Mathsoft Inc., Cambridge, MA) using a least squares analysis ($\alpha = 0.05$).

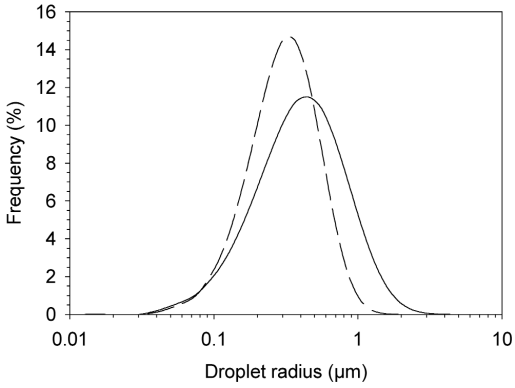

FIG. 1. Droplet size distributions of fat emulsified at 800/600 psi (—) and 2500/600 psi (– –).

RESULTS AND DISCUSSION

Homogeneous vs. heterogeneous nucleation models. The nucleation rate (J) in the bulk and emulsified systems was described by the following equation (12):

$$J = zn_s \nu e^{-E/kT} \exp(-16\pi\gamma^3 \upsilon_m^2 / 3\Delta s_m^2 kT\Delta T^2) \quad [1]$$

where z is the Zeldovich factor, n_s is the number of attachment sites at the nucleus surface, ν is a factor related to the molecular vibration frequency, E is the activation energy for the transport of molecules across the solid–liquid interface, υ_m is the molecular volume, Δs_m is the entropy of melting, k is the Boltzmann constant, γ is the Gibbs surface free energy, and T is temperature.

If homogeneous nucleation is considered to be first order and the droplet size distribution is accounted for, crystallization can be described with Equation 2:

$$\phi = 1 - \int_0^\infty \phi_d^0 \cdot \exp(-J \cdot t)\delta d \quad [2]$$

where ϕ is the volume fraction of crystallized droplets, J is the maximum rate of nucleation, t is time, and ϕ_d^0 represents the droplet volume distribution function (5,12).

Figure 2 shows the homogeneous nucleation rate for lard and PSCO as a function of undercooling ($1/T\Delta T^2$). The homogeneous nucleation rate for the PSCO blend was greater than in lard at both homogenization pressures, largely due to a greater undercooling in the former. The calculated J was found to be greater for emulsions formed at 800 psi than those formed at 2500 psi. The homogenization pressure effect shows that an increase in droplet number and surface-to-volume ratio resulted in a decrease in the nucleation rate of the system.

Homogeneous nucleation theory is typically inadequate for commercial fats, as they contain impurities that can affect nucleation and growth. Under such conditions, nucleation events may be accelerated by impurities followed by a retarded growth phase due to the poisoning of the crystal face. In emulsified fats,

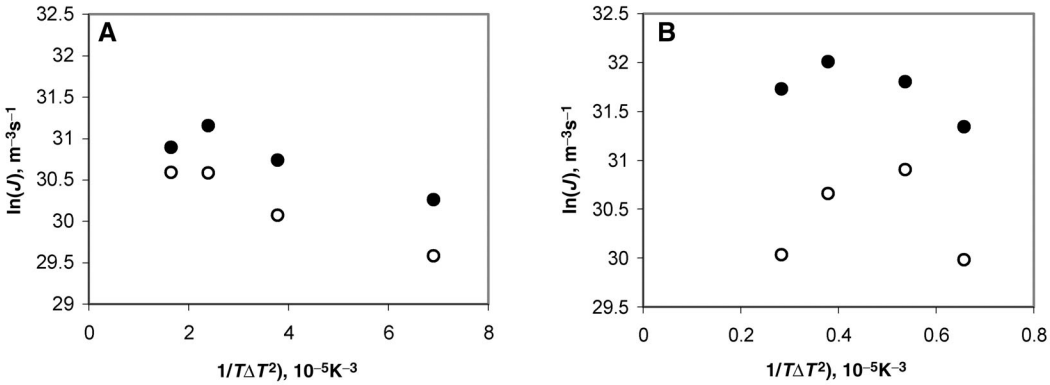

FIG. 2. Maximum homogeneous volume nucleation rate (J) as a function of undercooling ($1/T\Delta T^2$) for 40% lard (A) and palm stearin/canola oil (PSCO) (B) emulsions homogenized at two pressures: (●) 800 and (○) 2500 psi.

droplets that would otherwise have taken a considerable amount of time to nucleate by a homogeneous mechanism can nucleate quickly by a heterogeneous mechanism. The crystallization rate of emulsified fat in the presence of impurities is modeled by considering the crystallization rate (J) and the number of impurities present in the system (13):

$$\phi = 1 - \exp\left[-a(1 - e^{-Jt})\right] \quad [3]$$

where a is defined as the average number of impurities per droplet, and ϕ is defined as the volume fraction at time t. The relationship between impurities and volume fraction of the solidified fat can be described as

$$\phi_{max} = 1 - \exp(-a) \quad [4]$$

where ϕ_{max} is the maximum volume fraction of solid fat and a is the average number of impurities per droplet (13). Modeling of the crystallization curves for lard and PSCO using Equation 3 indicates a lower nucleation rate in the 2500- than the 800-psi treatments as a function of undercooling (Fig. 3).

Calculation of the number of impurities in the emulsified systems was dependent on the homogenization regime and on the type of fat (Fig. 4). The model predicted that less than one impurity was present per droplet in all systems. However, more impurities were present in the PSCO system than in the lard system. Impurity calculations indicated little difference between homogenization regimes in the PSCO system. Nevertheless, in both systems, the probability of a droplet containing more than one impurity was greater in the 800-psi treatment, given the presence of larger droplets. Increased impurity activity at lower homogenization pressures suggests that the droplet surface-to-volume ratio has a significant effect on the nucleation rate of the system. These results also show that nucleation could not be uniquely attributed to either homogeneous or heterogeneous nucleation, but rather to both. Had the average number of impurities per droplet been equal to one or more, heterogeneous nucleation would have been the dominant, and potentially sole, nucleation mechanism.

The dispersion of impurities decreased the ϕ_{max} for each system according to Equation 4 (Fig. 5). This was observed with lower ϕ_{max} values at each temperature studied for the

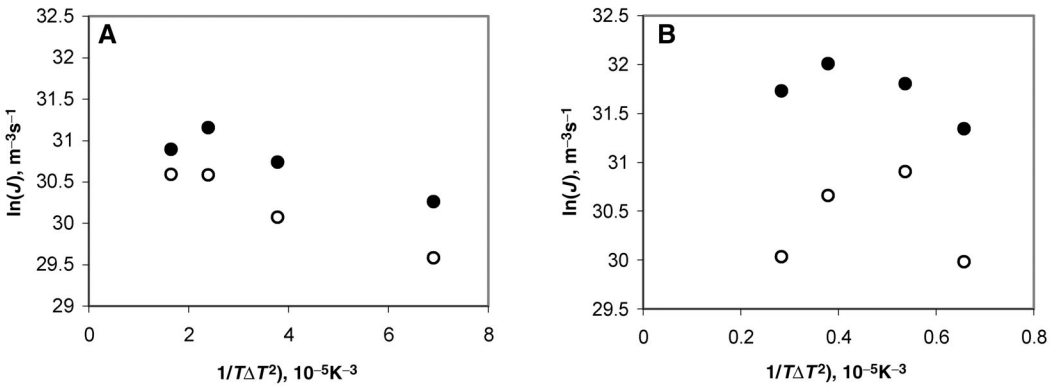

FIG. 3. Maximum heterogeneous volume nucleation rate (J) as a function of undercooling ($1/T\Delta T^2$) for 40% lard (A) and PSCO (B) emulsions homogenized at two pressures: (●) 800 and (○) 2500 psi. For abbreviation see Figure 2.

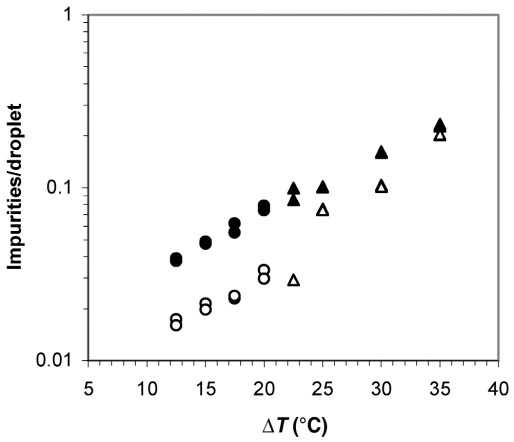

FIG. 4. Calculated number of impurities per droplet as a function of undercooling for lard emulsified at (●) 800 and (○) 2500 psi, and PSCO emulsified at (▲) 800 and (△) 2500 psi. For abbreviation see Figure 2.

2500-psi treatment relative to the 800-psi treatment. Dispersion of impurities into smaller droplets resulted in isolation of the catalytic sites and a decrease in the volume of fat affected by each impurity.

To determine which nucleation mechanism best represented the crystallization events in the emulsified fats, the physical properties of the emulsions were considered. With homogeneous nucleation, each droplet will nucleate individually and according to the same mechanism; as such, the extent of crystallization in the 800- and 2500-psi emulsions should be similar. The effect of homogenization was clear-cut in the case of lard, as the increase in the degree of dispersion in the system had a considerable effect on the ϕ_{max} of the system, with the 2500-psi treatment resulting in much lower values of ϕ_{max} than the 800-psi emulsions (Fig. 5A). This decrease indicated that the number of catalytic impurities was limiting. Thus, nucleation was heterogeneous in nature, and the dispersion of impurities played a large role in the crystallization kinetics of this system. Owing to the low degree of undercooling, homogeneous nucleation was not favorable. The PSCO emulsions were only somewhat sensitive to the degree of undercooling as well as the degree of dispersion (Fig. 5B). The relative insensitivity of the emulsions to the degree of dispersion indicated that nucleation partially occurred *via* a homogeneous mechanism or due to the presence of a critical concentration of impurities, with the latter being more likely unless substantial undercooling was applied to the system (e.g., 22.5 to 35°C).

Overall, the fit of the data for the lard and PSCO data showed that the heterogeneous model fit the data significantly better ($P < 0.05$) than the homogeneous model. As an example, graphical representation of the volume fraction vs. time is shown for lard in Figure 6.

The slope of the plot of ln(J) as a function of $1/(T\Delta T^2)$ is proportional to the Gibbs surface energy (γ) of the nuclei in the emulsion droplets (Figs. 2 and 3). The surface free energy of the 800-psi lard emulsion was calculated at 2.3 and 2.7 mJ·m^{-2} for the homogeneous and heterogeneous models, respectively. The γ calculated for the 2500-psi lard emulsions were 2.6 and 3.0 mJ·m^{-2}, respectively. As may be expected, the energy barrier to nucleation was greater in the finer emulsion due to a decrease in the effective volume available to be influenced by impurities.

For the PSCO treatment, a plot of ln(J) as a function of the undercooling term $1/T\Delta T^2$ was linear for only the homogeneous model. The heterogeneous model showed an initial increase in nucleation rate up to 20°C, followed by a decrease in nucleation rate at temperatures of 25 and 27.5°C. This was attributed to a polymorphic transition observed at lower temperatures (Fig. 7). Thus, γ was not calculated for this system. Calculated with the homogeneous model, γ yielded values of 4.2 and 6.1 mJ·m^{-2} for the 800- and 2500-psi treatments, respectively.

Avrami model. TAG crystallization behavior can be modeled using microscopic or numerical approaches (2). The Avrami model takes a form similar to the homogeneous model,

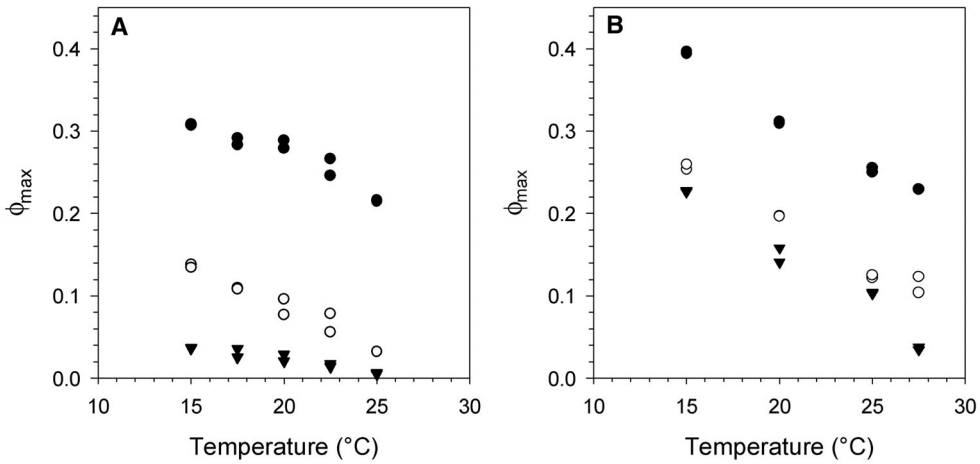

FIG. 5. Maximum volume fraction of solid fat (ϕ_{max}) for bulk and emulsified lard (A) and PSCO (B). Bulk (●), 800 psi (○), and 2500 psi (▼). For abbreviation see Figure 2.

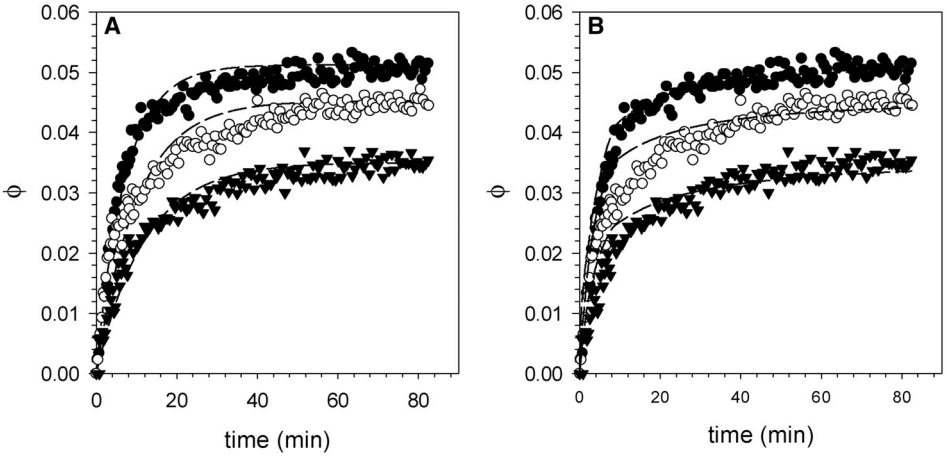

FIG. 6. Curve fits of lard emulsified at 800 psi for heterogeneous (A) and homogeneous (B) nucleation models at (●) 17.5, (○) 20, and (▼) 22.5°C.

with the solid fraction of fat expressed as a function of the ratio of solid fat content at time t, SFC(t), and solid fat content at time equal to infinity, SFC(∞), with an additional parameter n (the Avrami index) (14–17):

$$\frac{\text{SFC}(t)}{\text{SFC}(\infty)} = 1 - \exp(-kt^n) \quad [5]$$

Higher values of n indicate a greater dimensionality of nucleus growth (progressing from rodlike to disklike to spherulitic) or a change in mechanism from instantaneous to progressive or sporadic nucleation. This model can be used to describe crystallization within droplets but is of limited use, as it does not account for the distribution of droplet sizes encountered.

The Avrami index, n, of the bulk fats was strongly dependent on temperature, with n increasing significantly ($P < 0.05$) as a function of temperature, most notably in the PSCO system (Fig. 8). However, the model did not account for the differences between droplet size distributions generated *via* the two homogenization regimes, and was likely skewed toward the behavior of the larger droplets. Comparison of the Avrami indices of the emulsified and bulk lard showed that there were no significant differences ($P > 0.05$) between the emulsified and bulk treatments. At higher temperatures, the emulsified PSCO systems had smaller Avrami indices than in bulk ($P < 0.05$). Assuming that the Avrami index is an indicator of the dimensionality of growth within the droplet and an indicator of the nucleation mechanism, instantaneous nucleation occurred and smaller, less-ordered nuclei existed within the droplets. These differences in the bulk and emulsified behavior of n for both fats imply a difference in crystal morphology or nucleation behavior induced *via* emulsification, which may control crystal geometry and the location of nucleation. This is not overly surprising, as crystal diameters observed in bulk fats can easily approach the diameter of the droplets generated in these experiments. Limitations placed on the volume of substrate available for the diffusion, crystallization, and growth of crystals may therefore be expected to influence the Avrami index (17).

Crystallization rates (k) were lower for the emulsified treatments in both fat systems relative to their bulk counterparts (Fig. 9). In the lard, the Avrami constants decreased when lard was emulsified at 800 or at 2500 psi. The rate constants of both emulsification treatments were significantly lower than that of the bulk lard ($P < 0.05$).

The rate constants for the emulsified PSCO treatments were also significantly lower than in the bulk ($P < 0.05$). The Avrami constants for the PSCO systems at 15°C were lower than expected, increasing at 20°C before decreasing as temperature was increased to 27.5°C. A polymorphic transition or secondary crystallization event was likely responsible early in the crystallization process. As a result, limitations were encountered when fitting the Avrami model to the PSCO data at low temperatures. The consequence of this plateau was an underestimation of the crystallization rate and possible overestimation of k. The Avrami model is best suited to the analysis of monotropic systems or to the portion of the crystallization curve prior to the secondary crystallization event.

A discussion of the nucleation mechanism is difficult to pursue based on the Avrami model results, as microscopic evidence

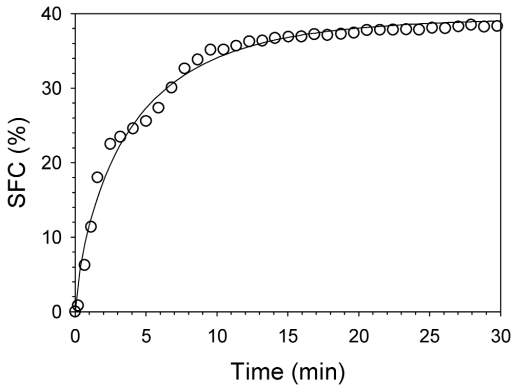

FIG. 7. Crystallization curve of PSCO at 15°C. SFC, solid fat content. For other abbreviation see Figure 2.

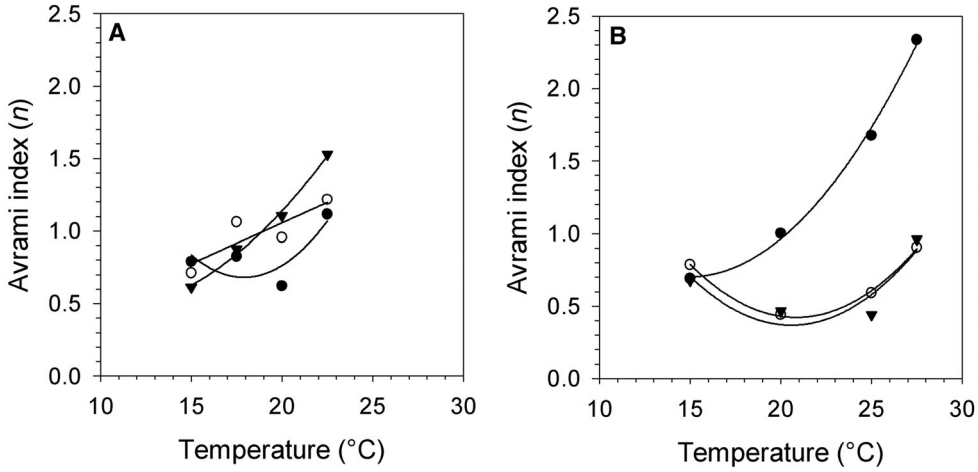

FIG. 8. Temperature dependence of the Avrami index (*n*) in emulsified mixtures. Lard (A) and PSCO (B) at homogenization pressures of (○) 800 and (▼) 2500 psi and (●) in bulk form. For abbreviation see Figure 2.

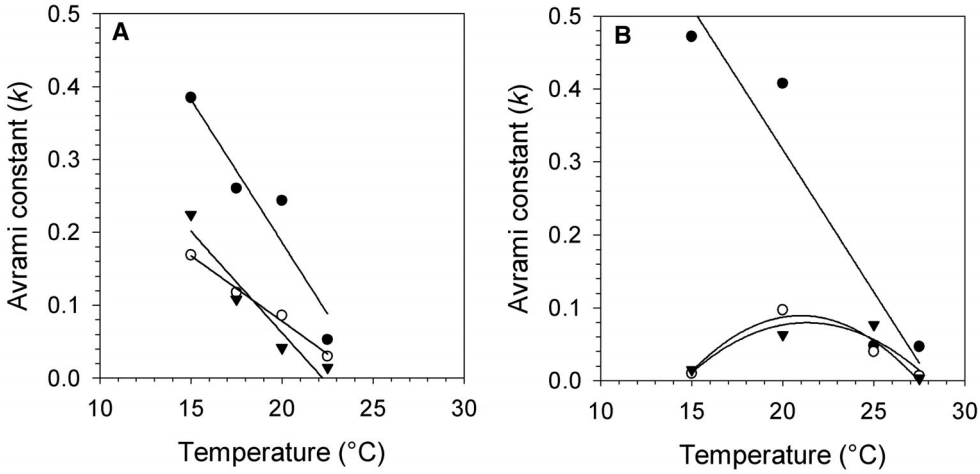

FIG. 9. The Avrami constant (*k*) as a function of temperature or as a function of undercooling. Lard (A) and PSCO (B) at homogenization pressures of (○) 800 and (▼) 2500 psi and (●) in bulk form. For abbreviation see Figure 2.

was not conclusive in these experiments (results not shown). Observation of the crystal microstructure in both the bulk and emulsified forms of the fats may provide useful insight into whether the forms of crystals within droplets are lending themselves to the lower Avrami indices relative to the bulk.

In conclusion, nucleation in bulk fat is expected to be heterogeneous in nature, moving to a mixture of heterogeneous and possibly homogeneous nucleation in emulsified form. As impurities are dispersed within emulsion droplets, those containing impurities are expected to nucleate quickly *via* a heterogeneous mechanism, whereas those devoid of impurities may be expected to nucleate homogeneously given sufficient undercooling. The barrier to nucleation is far lower in droplets that contain impurities; hence, they might be expected to nucleate rapidly, followed by the droplets that have the appropriate chemical potential for nucleation *via* homogeneous nucleation.

According to the Avrami model, the crystallization behavior of fat is modified by emulsification. The Avrami index remained low relative to the bulk fats. The rate of crystallization was also lowered in the emulsified systems for PSCO and lard emulsified at 800 and 2500 psi. Application of homogeneous and heterogeneous nucleation models to the crystallization data of these systems indicated that the heterogeneous model was more suitable for the description of the data, although this model did not necessarily fully substantiate the mechanism of nucleation.

ACKNOWLEDGMENTS

We would like to acknowledge the Natural Sciences and Engineering Research Council of Canada (NSERC) and the Ryerson University Office of Research for their financial support of this research.

REFERENCES

1. Boistelle, R., Fundamentals of Nucleation and Crystal Growth, in *Crystallization and Polymorphism of Fats and Fatty Acids*, edited by N. Garti and K. Sato, Marcel Dekker, New York, 1988, pp. 189–226.
2. Rousset, P., Modeling Crystallization Kinetics of Triacylglycerols, in *Physical Properties of Lipids*, edited by A.G. Marangoni and S.S. Narine, Marcel Dekker, New York, 2002, pp. 1–35.
3. Hindle, S., M.J.W. Povey, and K. Smith, Kinetics of Crystallization in *n*-Hexadecane and Cocoa Butter Oil-in-Water Emulsions Accounting for Droplet Collision Mediated Nucleation, *J. Colloid Interface Sci. 232*:370–380 (2000).
4. Skoda, W., and M. Van den Tempel, Crystallization of Emulsified TAGs, *J. Colloid Sci. 18*:568–584 (1963).
5. Kloek, W., P. Walstra, and T. van Vliet, Nucleation Kinetics of Emulsified Triglyceride Mixtures, *J. Am. Oil. Chem. Soc. 77*:643–652 (2000).
6. Walstra, P., and E.C.H. van Beresteyn, Crystallization of Milk Fat in the Emulsified State, *Neth. Milk Dairy J. 29*:35–65 (1975).
7. Awad, T., Y. Hamada, and K. Sato, Effects of Addition of Diacylglycerols on Fat Crystallization in Oil-in-Water Emulsions, *Eur. J. Lipid Sci. Technol. 103*:735–741 (2001).
8. Kaneko, N., T. Horie, S. Ueno, J. Yano, T. Katsuragi, and K. Sato, Impurity Effects on Crystallization Rates of *n*-Hexadecane in Oil-in-Water Emulsions, *J. Crystal Growth 197*:263–270 (1999).
9. Hodate, Y., S. Ueno, J. Yano, T. Katsuragi, Y. Tezuka, T. Tagawa, N. Yoshimoto, and K. Sato, Ultrasonic Velocity Measurement of Crystallization of Palm Oil in Oil-in-Water Emulsions, *Colloids Surf. A, 128*:217–224 (1997).
10. Campbell, S.D., H.D. Goff, and D. Rousseau, Comparison of Crystallization Properties of a Palm Stearin/Canola Oil Blend and Lard in Bulk and Emulsified Form, *Food Res. Int. 35*:935–944 (2002).
11. *Official Methods and Recommended Practices of the AOCS*, 5th edn., AOCS Press, Champaign, 1997.
12. Kashchiev, D., N. Kaneko, and K. Sato, Kinetics of Crystallization in Polydisperse Emulsions, *J. Colloid Interface Sci. 208*:167–177 (1998).
13. Kashchiev, D., D. Clausse, and C. Jolivet-Dalmazzone. Crystallization and Critical Supercooling of Disperse Liquids, *Ibid. 165*:148–153 (1994).
14. Avrami, M., Kinetics of Phase Change I. General Theory, *J. Chem. Phys. 7*:1103–1112 (1939).
15. Avrami, M., Kinetics of Phase Change II. Transformation–Time Relations for Random Distribution of Nuclei, *Ibid. 8*:212–224 (1940).
16. Sharples, A., Overall Kinetics of Crystallization, in *Introduction to Polymer Crystallization*, Edward Arnold, London, 1966, pp. 44–59.
17. Kashchiev, D., *Nucleation: Basic Theory with Applications*, Butterworth-Heinemann, Oxford, 2000, pp. 366–368.

[Received October 17, 2002; accepted December 24, 2003]